

DAA/ LANGLEY

IN-24

69600 CR

P.33

RO 935

**SEMI-ANNUAL PROGRESS REPORT**

**NASA GRANT NAG-1-253**

**SUBMITTED MAY 15, 1987**

**A MICROGRAPHIC STUDY OF BENDING FAILURE IN FIVE  
THERMOPLASTIC/CARBON FIBER COMPOSITE LAMINATES**

**BY**

**S.W. Yurgartis and S.S. Sternstein  
Rensselaer Polytechnic Institute  
Materials Engineering Department  
Troy, New York 12180-3590**

**(NASA-CR-180537) A MICROGRAPHIC STUDY OF  
BENDING FAILURE IN FIVE THERMOPLASTIC/CARBON  
FIBER COMPOSITE LAMINATES Semiannual  
Progress Report (Rensselaer Polytechnic  
Inst.) 33 p Avail: NIS HC A03/MF A01**

**N87-26147**

**Unclas  
0069600**

**G3/24**

## ABSTRACT

The local deformation and failure sequences of five thermoplastic matrix composites were microscopically observed while bending the samples in a small fixture attached to a microscope stage. The thermoplastics are polycarbonate, polysulfone, polyphenylenesulfide, polyethersulfone, and polyetheretherketone. The composites made from these plastics contain a variety of carbon fibers, though all with similar properties, and have fiber volume fractions ranging from 32% to 66%. Comparison is made to an epoxy matrix composite, 5208/T-300. Laminates tested are  $(0/90)_2S$ , with outer ply fibers parallel to the beam axis. Four point bending is used at a typical span-to-thickness ratio of 39:1. A shallow notch is put in the samples at mid-span to avoid failure under the loading pins. It was found that all of the thermoplastic composites failed by abrupt longitudinal compression buckling of the outer ply. Very little precusory damage was observed. Micrographs reveal typical fiber kinking associated with longitudinal compression failure. Curved fracture surfaces on the fibers suggest they failed in bending rather than direct compression. Delamination was suppressed in the thermoplastic composites, and the delamination that did occur was found to be the result of compression buckling, rather than visa-versa. Microbuckling also caused other subsequent damage such as ply splitting, transverse ply shear failure, fiber tensile failure, and transverse ply cracking.

## 1. Introduction

Present day composites made from lamina of continuous carbon fibers embedded in a polymeric matrix tend to be particularly susceptible to damage from out-of-plane loads, such as projectile impact. Delamination tends to occur, causing a substantial reduction in in-plane properties, such as compression strength.<sup>(1)</sup>

The search for high performance composites with improved damage tolerance has prompted speculation that substitution of the relatively brittle thermoset matrices currently in use with relatively ductile thermoplastic matrices might lead to better delamination resistance and thus better subsequent in-plane residual strength after impact. Unfortunately, the relationships among fiber properties, bulk matrix properties, composite microstructural parameters, and composite damage tolerance capabilities remain uncertain. Also uncertain are the trade-offs against other composite properties that may have to be made in the effort to produce tougher composites, for example creep resistance, solvent resistance, service temperature, stiffness, and so on.

In this light, out-of-plane loading experiments which help to reveal the nature of local deformations and failures in a variety of composites, and then try to correlate these with constituent properties, seem desirable. The results reported herein are primarily a qualitative study of thermoplastic matrix composite failures. An attempt to quantify these failures and relate them to constituent properties is in progress.

The deformation and failure of five different thermoplastic

matrix composites subjected to four-point bending are microscopically examined in-situ. Bending is used as an approximation of out-of-plane loading, but it should be noted that bending does not include the out-of-plane normal stresses that accompany projectile impacts. The thermoplastics studied have a wide range of mechanical properties. The fibers in these composites, although not identical, have similar properties. Thus this study looks at the role that matrix properties play in composite behavior. Comparisons are made to a benchmark epoxy matrix composite, namely 5208/T-300.

## 2. Materials

Table 1 lists the materials used in this work. Laminates are made in our laboratory from prepreg supplied to us from various sources. Most of the laminates tested are eight ply, (0/90)<sub>2S</sub>.

Laminates are made by pressing prepreg layers between two polished plattens, with shims inserted at the platten edges to prevent overpressing. Processing temperatures are: PC-240°C, PPS-320°C, PS-315°C, PES-340°C, PEEK-380°C. Typically 100 psi is applied for 5 minutes. Semicrystalline matrix composites (PPS and PEEK) are cooled quickly by transferring the entire stack to a room temperature press. The measured fast cooling rate at the center of the laminate is approximately 11.3 °C/s. Amorphous matrix composites are cooled slowly in the press, where the cooling rate is  $\frac{dT}{dt} = 2(10)^{-4}(T-20)$  °C/s. Some PPS laminates were also given an annealing treatment, as noted below. The 5208 laminate was supplied to us fully cured.

Small beam samples are cut from the laminate so that the outerply fiber direction is parallel to the beam long axis. As is discussed below, it is found necessary to notch the midsection of the samples; this is done with a diamond-grit routing tool.

The four types of fibers involved all have similar diameter (ca.  $7\mu\text{m}$ ) and similar tensile properties: modulus  $\sim 230$  GPa, strength  $\sim 3$  GPa, strain-at-failure  $\sim 1.4\%$ . Table 2 gives approximate values for some of the mechanical properties of the bulk matrix materials. Caution must be used when looking at the values in Table 2, since the stress-strain behavior of these materials is complex, non-linear, and subject to many variables such as prior thermal history and strain rate. Nonetheless, Table 2 does indicate the range of properties represented by the matrix materials of this study.

### 3. Experimental

#### 3.1 Test Geometry and Procedure

Beam samples are bent in a small 4-pt bending fixture. The fixture uses 4.76 mm diameter loading pins; the outer support span is 39 mm, and the inner loading pins are at one third the span distance. Typical span-to-thickness ratio of the samples is 39:1.

It was found that unnotched samples (except 5208/T-300) invariably failed underneath, or adjacent to, the central loading pins. This was true despite attempts to distribute the contact load by use of various shims. The difficulty was overcome by notching the samples. Figure 1 shows the sample geometry. It

is believed preferable to have minor and consistent stress concentrations introduced by a shallow notch rather than the artifactual failures due to high contact stresses at the loading pins. Our experience points to the caution that must be used when interpreting flexure data of similar materials in the literature.

The bending fixture is mounted on a microscope stage and a sample with a polished flat edge (opposite the notched side) is observed by reflected light microscopy while being deformed. Sample deflection is accomplished by hand via a micrometer screw and barrel, and thus the deflection can be measured, but the deformation rate is uncontrolled, slow, and incremental, with pauses made for observation and photography. Load is not measured.

In a modification of the experiment, the same bending fixture is mounted in a screw Instron machine. Doubly notched samples (on opposite sides, with 1 mm deep notches) are bent at a crosshead rate of 2 mm/min while the load and beam center deflection are measured, the later by an extensometer arm below the sample midsection.

All experiments reported here are at room temperature. A minimum of four samples of each material were tested. More than 25 PEEK composite samples were tested. The micrographs presented were chosen to be representative of typical material behavior; an attempt is made to note significant variations in the discussion.

Fiber volume fraction measurements are made by the point intercept technique applied to micrographs of one representative

sample of each material; results are shown in Table 1. Notice the low fiber volume fraction (32%) of the polycarbonate composites.

### **3.2 Preparation of Micrographs**

The micrographs presented below are of samples that have failed, been removed from the bending fixture, and potted in an epoxy mounting medium. This allows sectioning of the sample and results in a more photogenic view of the failure due to depth-of-field limitations in microscopy. However the basic features of edge viewed samples and subsequently sectioned samples are the same.

Polishing of the sample is adapted from standard metallographic techniques. Simple non-polarized reflected light microscopy is employed; micrographs are made on Kodak 135 Technical Panchromatic 2415 film with a 550 nm bandpass filter at the illumination source. Fibers appear white in the micrographs, and distinction between the composite matrix and the epoxy mounting medium is revealed as a slight difference in grey tone. An approximate magnification scale sufficient for the purpose of this paper is available by recognizing that a fiber diameter is about 7 $\mu$ m.

## **4. Results and Discussion**

### **4.1 Longitudinal Compression Failure in Bending**

All of the thermoplastic-based composites failed catastrophically by longitudinal compression failure at the outer ply. Micrographs, Figures 2-6, show typical bending compression failures of the five thermoplastic composites. Shown are the

outer ply failures; the second transverse ply is also seen. In contrast, the compression region of a 5208 composite that has failed, though not shown, reveals no damage, but instead these samples fail in tension, as discussed below.

The bending compression failures are generally abrupt, accompanied by a loud snap. Faint crackling noises are sometimes heard prior to catastrophic failure; however, little precursory damage is observed microscopically. Occasionally a few fiber breaks in the outer tensile ply are seen prior to failure, and occasionally transverse cracks open in the first 90° tension ply, but this damage does not appear to significantly influence the compression failure.

Some slight time dependence - manifest as a delay between an increment in deformation and eventual failure - was occasionally found in all materials, indicating that yielding is occurring somewhere. However, we were never able to observe the locus of this yielding microscopically. Careful observation of the anticipated failure region did not reveal any cracking or yielding prior to catastrophic failure.

It must be noted that only the unnotched side of the sample was being observed. On the other side, stress concentration at the notch may result in initial yielding or failure of the beam. Unfortunately it was not possible to observe the notched region of the sample in-situ. However, subsequent to the sample failure, the microscopic failure appearance was found to be uniform across the width of the beam. In addition, not all failures occurred

at the root of the notch. These results, along with the noted abruptness of the failures, lead us to cautiously conclude that the in-situ microscopic observations at the unnotched edge are representative of the material behavior, with or without the mild notch.

Failure stresses, estimated from simple beam theory as applied to laminated plates and assuming a simple reduction in cross-section at the notch, lend further support to this conclusion: compression failure stresses in the notched PEEK/XAS beams so calculated are greater than the failure stresses of the same material in unnotched direct compression tests. Clearly, any consideration of a stress concentration factor at the notch would serve to increase the calculated failure stresses in the notched beams. It is therefore reasonable to conclude that the mild notch does not alter appreciably the observed failure pattern.

#### **4.2 Load-Deflection Curves**

Typical load-deflection curves for the various materials are shown in Figure 7. The failures appear to be abrupt, although small load drops are found occasionally prior to failure, and are correlated to the noises noted earlier. For 8-ply samples, failures occur at center deflection to thickness ratios that range from 4.3:1 to 2.3:1. The decreasing slope of the load-deflection curves at larger deflections (hereafter referred to as softening) can be partly attributed to the inherent non-linearity of the bending geometry as deflections approach the beam thickness. There are also material nonlinearities which may be quite important.

Softening of longitudinal compression modulus has been observed for numerous composite systems.<sup>(2)</sup> This is contrary to the well-known hardening of compression modulus (and softening of tensile modulus) in neat polymers due to free volume effects. In fact, a recent paper<sup>(3)</sup> addresses similar effects for ceramics and the resultant nonlinearities which derive from different tensile and compressive creep rates in a bending geometry. Presumably, in the case of composites, softening of longitudinal compression modulus may be due to local non-axial fiber deformations (bending), that is, an increase in fiber waviness amplitude.

#### **4.3 Kink Morphology**

Figures 2-6 all show localized fiber buckling typical of longitudinal compression failure in fibrous composites.<sup>(4-6)</sup> Short fiber fragments, characteristic of what is called "kinking" or microbuckling, are seen in all the figures, even the PC and PPS samples which also show large bending deformations of the fibers as well. The ratio of the length of these fiber fragments to the fiber diameter ranges from about 11:1 to 1:1, with a typical value of approximately 5:1. This is in the range reported by other workers, although the observations by others are for direct compression tests, rather than bending.<sup>(2)</sup> Not enough data is available here to permit quantitative comparisons between the fragment lengths of different materials. Qualitatively, however, it can be stated that the PEEK composites have the shortest, and least uniform, kink fragments.

The sigmoid shaped crack surfaces visible on some fiber ends suggest that the fibers have failed in bending, rather than in direct compression. This same geometry is seen in snapped glass rods. Schindler and coworkers<sup>(7)</sup> have modeled dynamic bending failure of simple beams, and find that cracks do turn to run parallel to the beam axis when a sufficient axial compressive stress is superposed on the bending stresses. In the present case, however, the inhomogeneous and anisotropic morphology of carbon fibers greatly complicates the problem.

#### 4.4 Delamination and Ply Splitting

Some minor delamination is observed in PEEK and PS samples, while intraply splitting is seen in the PEEK and PES materials. No significant delamination or ply splitting is found in PC or quenched PPS samples. The delamination that occurred did so after compression buckling initiated. This conclusion is supported by two types of observation. First, samples were carefully examined microscopically while they were slowly and incrementally displaced up to failure. No delamination, or evidence of incipient delamination, is found. Second, similar bending compression failures are found in a set of samples designed to suppress delamination. A  $[0/90]_{2S}$  laminate was prepared with an additional neat PEEK resin film inserted between the outer and second plies. Figure 8 shows the bending failure of a beam cut from this laminate. It is similar to Figure 6, but without delamination. For the materials tested in this study it appears that delamination (and

ply splitting) is the result of, rather than the cause of, compression failure.

The PES and PEEK samples showed a consistent tendency for ply splitting. In PES, ply splitting dominates and delamination is essentially absent; this may be due to the fairly high intraply void content, as seen in Figure 5. These voids often have high aspect ratios, and are due to poor resin impregnation during prepregging. It should also be noted that the PES composites have the highest fiber volume fraction of the samples tested; the closer fiber spacing may also contribute to the tendency for ply splitting.

While PEEK samples also showed ply splitting, the split was usually arrested within a distance of one to three ply thicknesses. Delamination did not usually exceed 1 to 3 mm on either side of the compression failure. In fact, none of the thermoplastic composites delaminated extensively, in contrast to the epoxy-based samples which sometimes delaminated to an end of the beam. The short, simple ply splitting of the PEEK samples and the absence of well developed kink fragments gives these samples the appearance of supporting high compression loads before failure.

#### **4.5 Transverse Shear Failure**

The shear failure of the transverse ply below the outer zero degree ply, as seen in Figure 5, is also typical of PEEK, PES, PS (and occasionally PPS) samples. This is also shown for a PEEK sample in Figure 8. Little yielding is observed in the transverse

plys of PEEK, PES, PS composites, while the transverse plys of PC and quenched PPS appear to tolerate fairly large local bending deformations. Compression failure often propagates to the third ply (the second longitudinal ply). Constraint by the material above and below this ply results in more uniform kinking behavior, as vividly illustrated for a PC composite in Figure 9.

#### **4.6 Accompanying Tensile Damage**

The tensile damage that accompanies compression failure of the thermoplastic composites varies widely from sample to sample, and only shows a weak trend among the different materials. Damage ranges from undetectable to moderate. Figures 10a and 10b show the range of tensile damage observed. Epoxy-based samples, conversely, failed by a combination of tensile and delamination damage; tensile failure of a 5208 sample is shown in Figure 11.

Tensile damage in the thermoplastic composites is probably the result of a dynamic fracture process that initiates upon compression collapse. The role that any substantial precursory tensile damage would have on incipient compression failure is unknown.

#### **4.7 Annealing of PPS Samples**

Another complexity in these materials is the influence of semicrystalline matrix morphology on composite properties. The effect of thermal treatment on PPS composites was briefly examined. Four PPS beam samples were annealed at 208°C for 2 hours; this schedule has been shown to result in maximum polymer crystallinity

in bulk PPS.<sup>(8)</sup> DTA traces confirmed the quenched samples had a much lower crystallinity than the annealed samples.

Sectioning and polishing of annealed untested samples reveals a large number of regularly spaced transverse cracks, particularly in the center plys. Some of these cracks are visible in Figure 12. Apparently the volume changes accompanying matrix crystallization result in high residual stresses. Annealing also affects bending failure. Two of the annealed samples failed by mid-beam delamination. The other two failed in bending compression, but unlike quenched samples, delamination and ply splitting occurred, and little deformation of the second ply is observed (see Figure 12).

## 5. Conclusions

The thermoplastic composites, when compared to an epoxy matrix composite such as 5208/T-300, appear to be successful at suppressing delamination failure in bending. For the five thermoplastic composites studied here the weakness in bending was longitudinal compression failure. In-situ microscopic examination revealed very little precursory cracking or yielding prior to catastrophic compression failure. Bending compression failures have the characteristic kink form often found in the direct compression failure of such composites. Individual fiber failures, however, appear to be due to bending.

The small amount of delamination that sometimes accompanies failure was a result of compression buckling, and not visa-versa. Other types of damage that occurred subsequent to compression

failure included ply splitting, transverse ply shear failure, and tensile failures such as broken fibers and transverse ply cracks.

As expected, thermal history had a marked effect on the mechanical properties of the semicrystalline PPS matrix composite. Annealing to achieve high crystallinity appears to result in high residual stresses.

The test geometry used in this work suggests that bending may be a convenient geometry for studying the longitudinal compression strength of some composites. The 0/90 layup is somewhat analogous to the honeycomb sandwich beams already used to study compression behavior, but here the soft mid-layer is more readily obtained with transverse plies in the layup. The stress concentration effect of the notch remains troublesome, but perhaps no more so than the stress concentrations encountered in other test geometries.

The challenge now is to understand why these thermoplastic composites are weak in compression. Our preliminary work along these lines suggests that a simple explanation, such as a proportionality between compression strength and matrix modulus, is insufficient for these materials.

#### **ACKNOWLEDGEMENTS**

This work is supported by the National Aeronautics and Space Administration under grant NAG-1-253. The authors are especially grateful to Dr. Norman Johnston for providing materials, guidance

and helpful discussions throughout this work. The PEEK and PES prepreg materials were supplied through the generosity of Dr. Neil Cogswell and Dr. Roy Moore of ICI.

ORIGINAL PAGE IS  
OF POOR QUALITY

REFERENCES

1. J.G. Williams and M.D. Rhodes, in Composite Materials: Testing and Design (Sixth Conference), ASTM STP 787, edited by I.M. Daniel (Am. Soc. for Testing and Materials, 1982), p.450.
2. H.T. Hahn and J.G. Williams, NASA Technical Memorandum 85834.
3. T. Chuang, J. Materials Science, 21 (1986), 165.
4. T.V. Parry and A.S. Wronski, J. Materials Science, 17 (1982), 893.
5. A.G. Evans and W.F. Adler, Acta Met., 26, (1978), 725.
6. M.R. Piggott and B. Harris, J. Materials Science, 15, (1980), 2523.
7. H.J. Schindler and M. Sayir, Intl. Journal of Fracture, 25, (1985), 95.
8. D.G. Brady, J. Appl. Polymer Science, 20, (1976), 2541.

TABLE & FIGURES CAPTIONS

- Table 1. Composite materials tested.
- Table 2. Approximate tensile properties of the matrix materials, at 20°C.
- 
- Figure 1. Micro-beam sample geometry.
- Figure 2. Bending compression failure of a polycarbonate/AS-4 carbon fiber composite showing a typical kink geometry.
- Figure 3. Bending compression failure of a quenched polyphenylene sulfide/C-6000 carbon fiber composite.
- Figure 4. Bending compression failure of a polysulfone/C-6000 carbon fiber composite. Notice curved fiber ends, suggesting fiber failure in bending.
- Figure 5. Bending compression failure of a polyethersulfone/XAS carbon fiber composite. Ply splitting is typical, as is transverse ply shear failure.
- Figure 6. Bending compression failure of a polyetheretherketone/XAS carbon fiber composite. Notice ply splitting and minor delamination.
- Figure 7. Typical load-deflection curves of composite micro-beam samples in 4 point bending.
- Figure 8. Bending compression failure in a PEEK/XAS composite, with an additional PEEK film added at the 1-2 ply interface to suppress delamination.
- Figure 9. Microbuckling failure of the third ply in a PC/AS-4 composite. Constraint by neighboring plies allows several kinks to form.
- Figure 10. Typical range of tensile damage subsequent to bending compression failure. Shown are PEEK/XAS samples.  
a) No apparent damage. b) Fiber tensile failure in outer ply. Crack in transverse ply, (note that crack is filled with potting resin).
- Figure 11. Bending tensile failure of a 5208 epoxy/T-300 carbon fiber composite. Delamination extends well beyond field of view.
- Figure 12. Bending compression failure in a PPS/C-6000 composite that has been annealed to produce high matrix crystallinity. Notice transverse cracks which are present before bending the sample. Compare failure to Figure 5.

TABLE 1.

MATRIX	FIBER	SUPPLIER	V <sub>f</sub>	AVG. 8 PLY THICKNESS (mm)
Polyetherether ketone (PEEK)	XAS	ICI	.57	1.10
Polyethersulfone (PES)	XAS	ICI	.65	1.05
Polysulfone (PS)	C-6000	NASA Langley	.57	1.09
Polyphenylenesulfide (PPS)	C-6000	Phillips Petroleum	.56	1.29
Polycarbonate (PC)	AS-4	NASA Langley	.32	1.59
Epoxy (5208)	T-300	NASA Langley	.60	1.63 (12 ply)

ORIGINAL PAGE IS  
OF POOR QUALITY

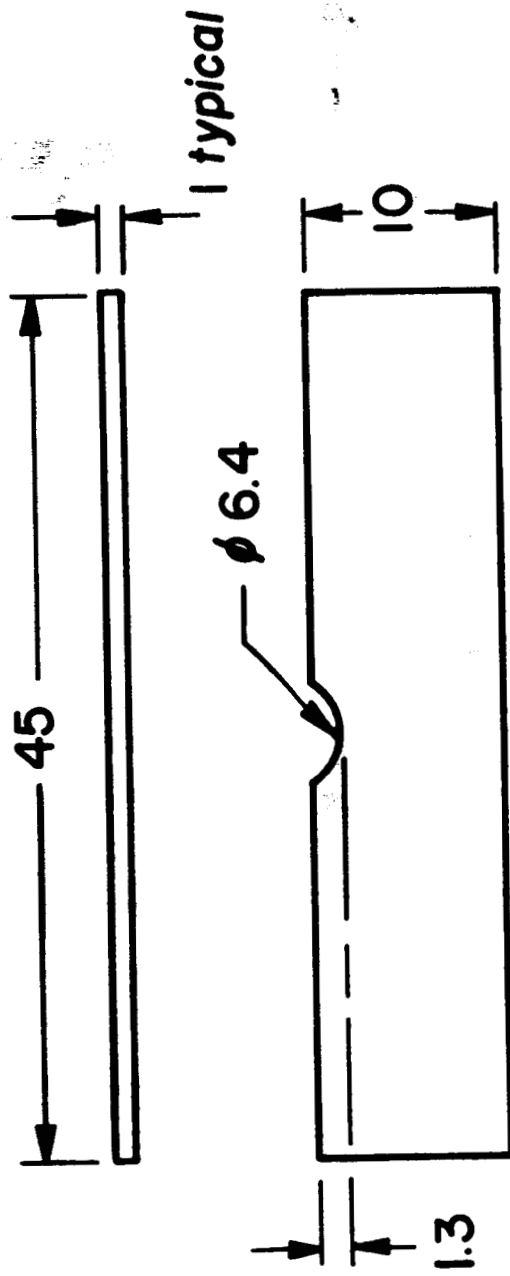
TABLE 2.

MATRIX	$\sigma_y$ (MPa)	$\epsilon_y$ (%)	E (GPa)
PC	62	7	2.4
PS	70	5	2.5
PEEK	100	6	3.5
PES	70	3.7	2.8
PPS	74	3	3.8
EPOXY (5208)	57	1.5	4.0

$\sigma_y$ ,  $\epsilon_y$  are yield stress, strain respectively. E = Young's modulus

ORIGINAL PAGE IS  
OF POOR QUALITY

ORIGINAL PAGE IS  
OF POOR QUALITY



All dimensions in mm

FIGURE 1.

ORIGINAL PAGE IS

ORIGINAL PAGE IS  
OF POOR QUALITY



FIGURE 2.

ORIGINAL PAGE IS  
OF POOR QUALITY

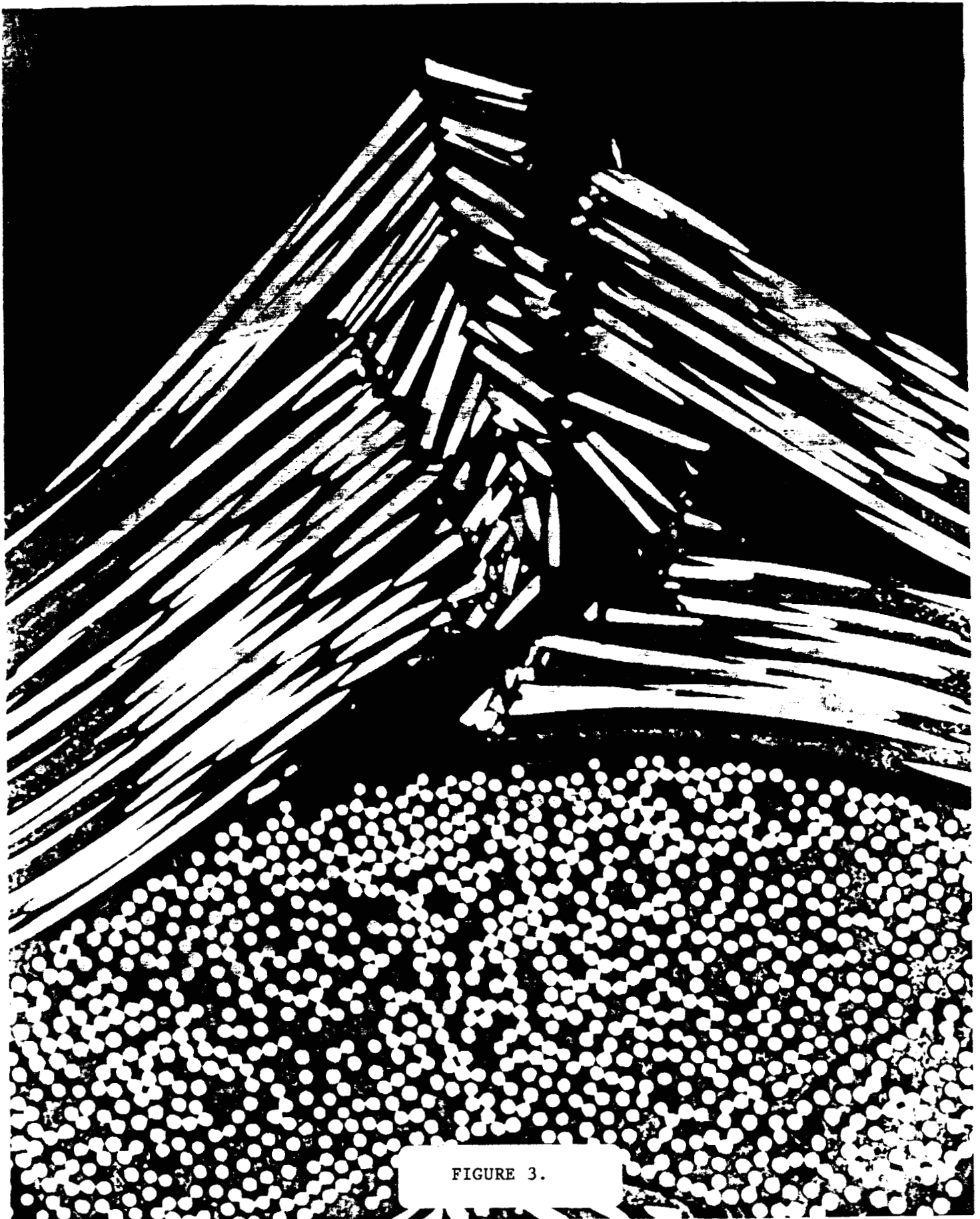


FIGURE 3.



FIGURE 4.

ORIGINAL PAGE IS  
OF POOR QUALITY

ORIGINAL PAGE IS  
OF POOR QUALITY



FIGURE 5.

ORIGINAL PAGE IS  
OF POOR QUALITY

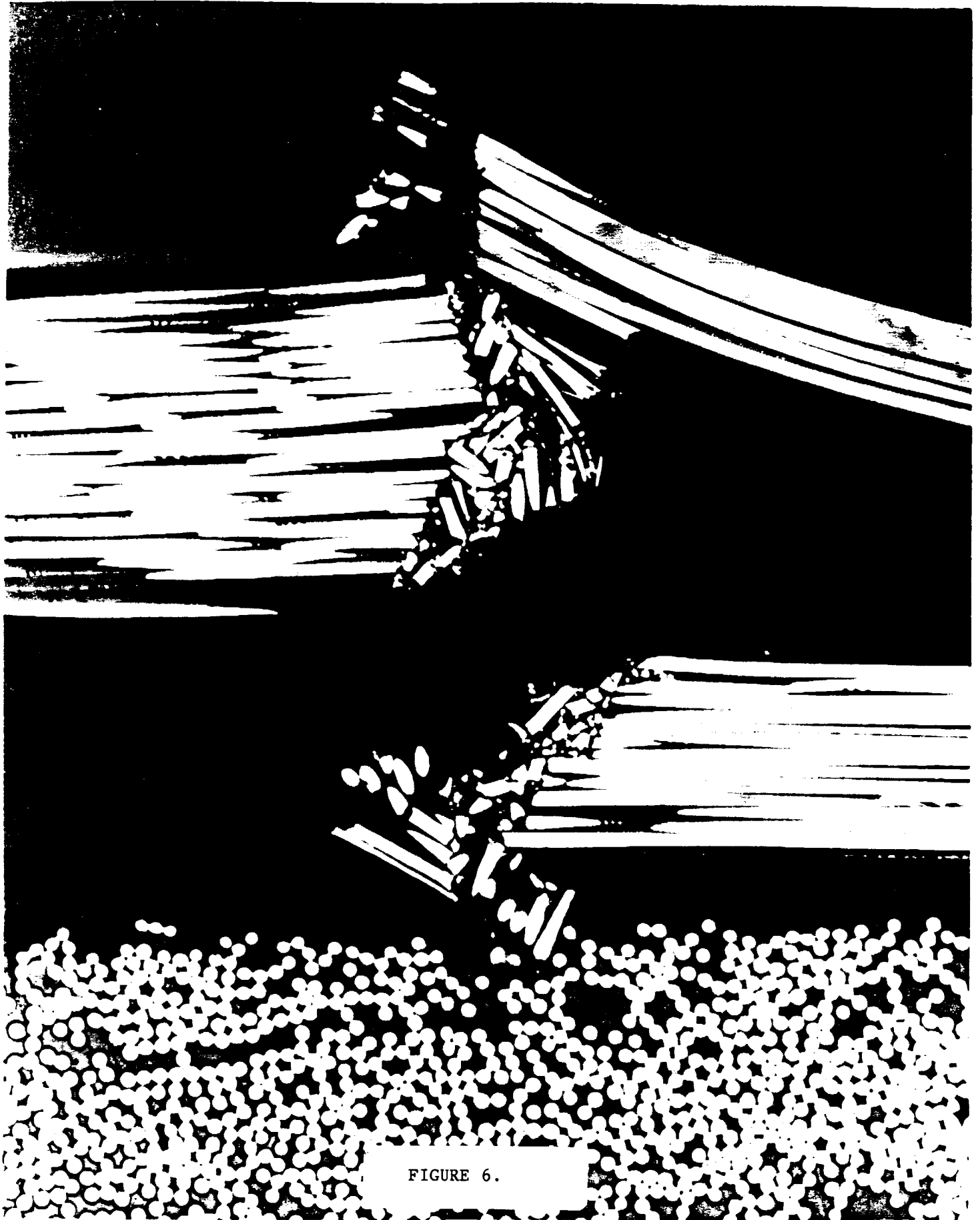


FIGURE 6.

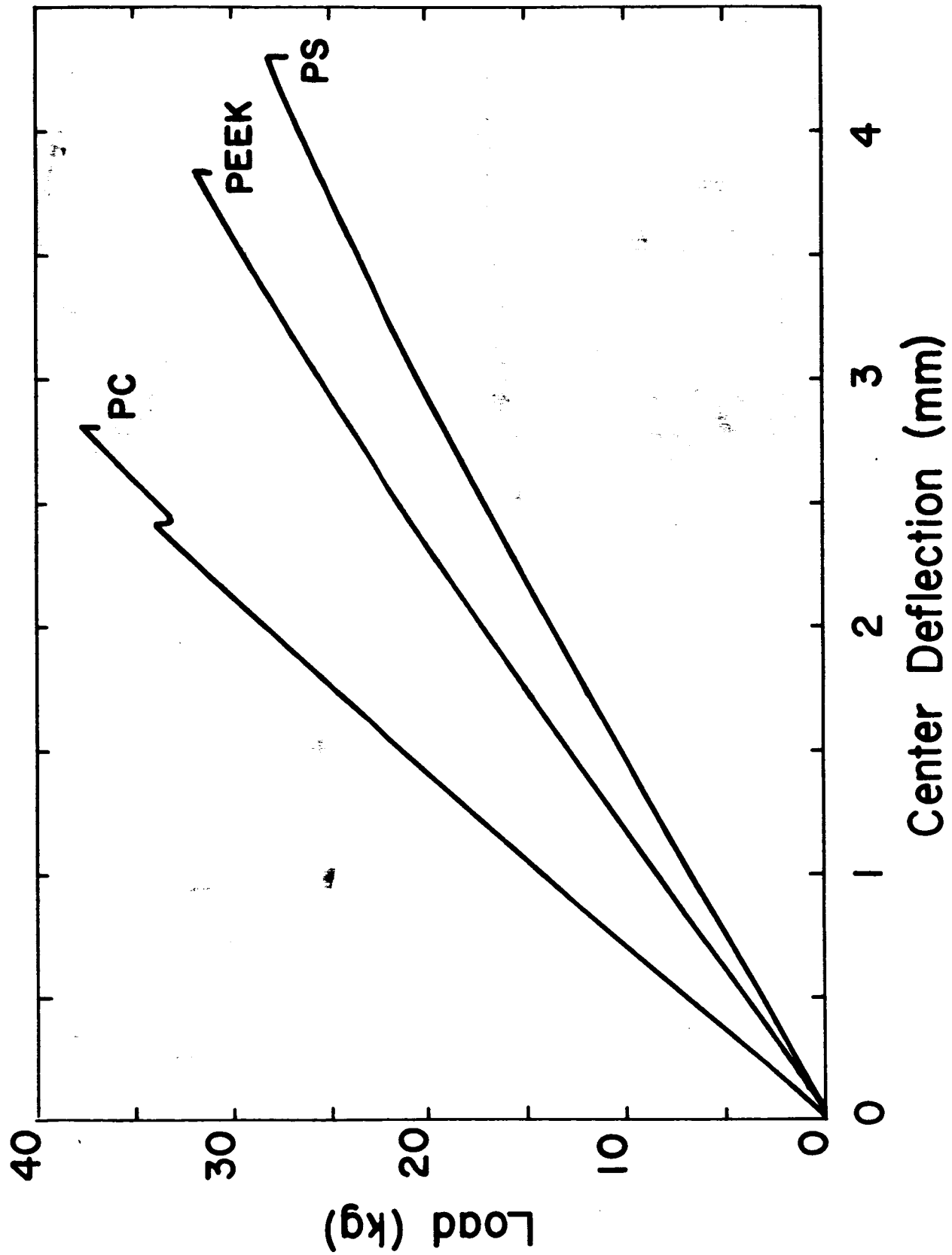


FIGURE 7.

ORIGINAL PAGE IS  
OF POOR QUALITY



FIGURE 8.

ORIGINAL PAGE IS  
OF POOR QUALITY.

ORIGINAL PAGE IS  
OF POOR QUALITY.



FIGURE 9.

ORIGINAL PAGE IS  
OF POOR QUALITY.

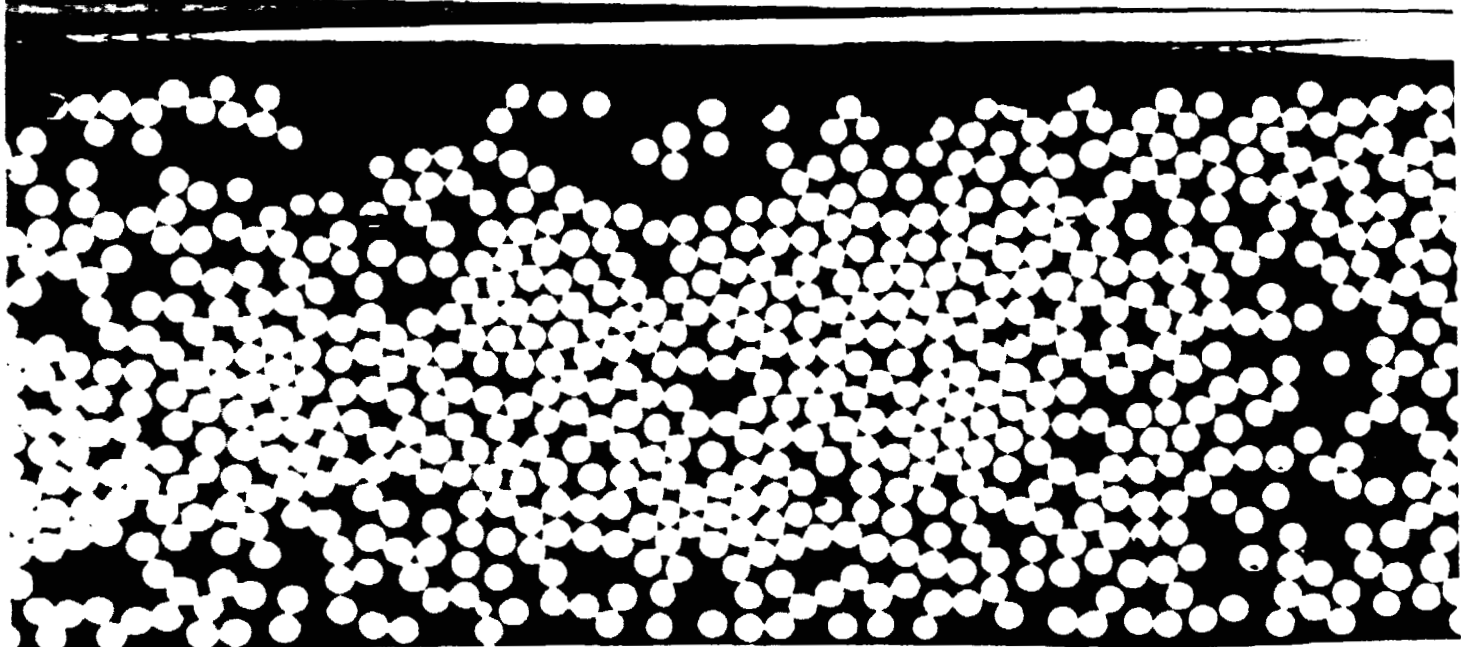
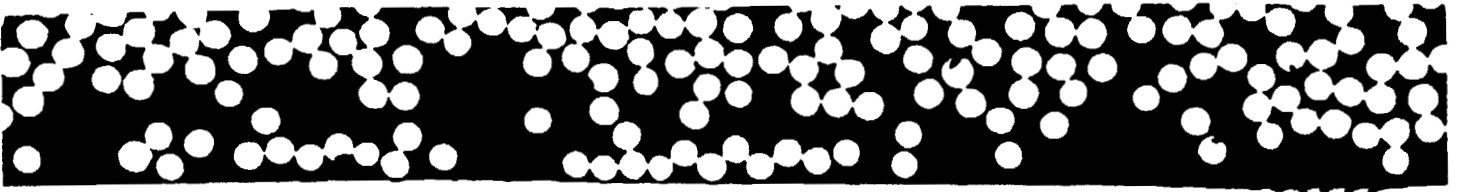


FIGURE 10a.

ORIGINAL PAGE IS  
OF POOR QUALITY

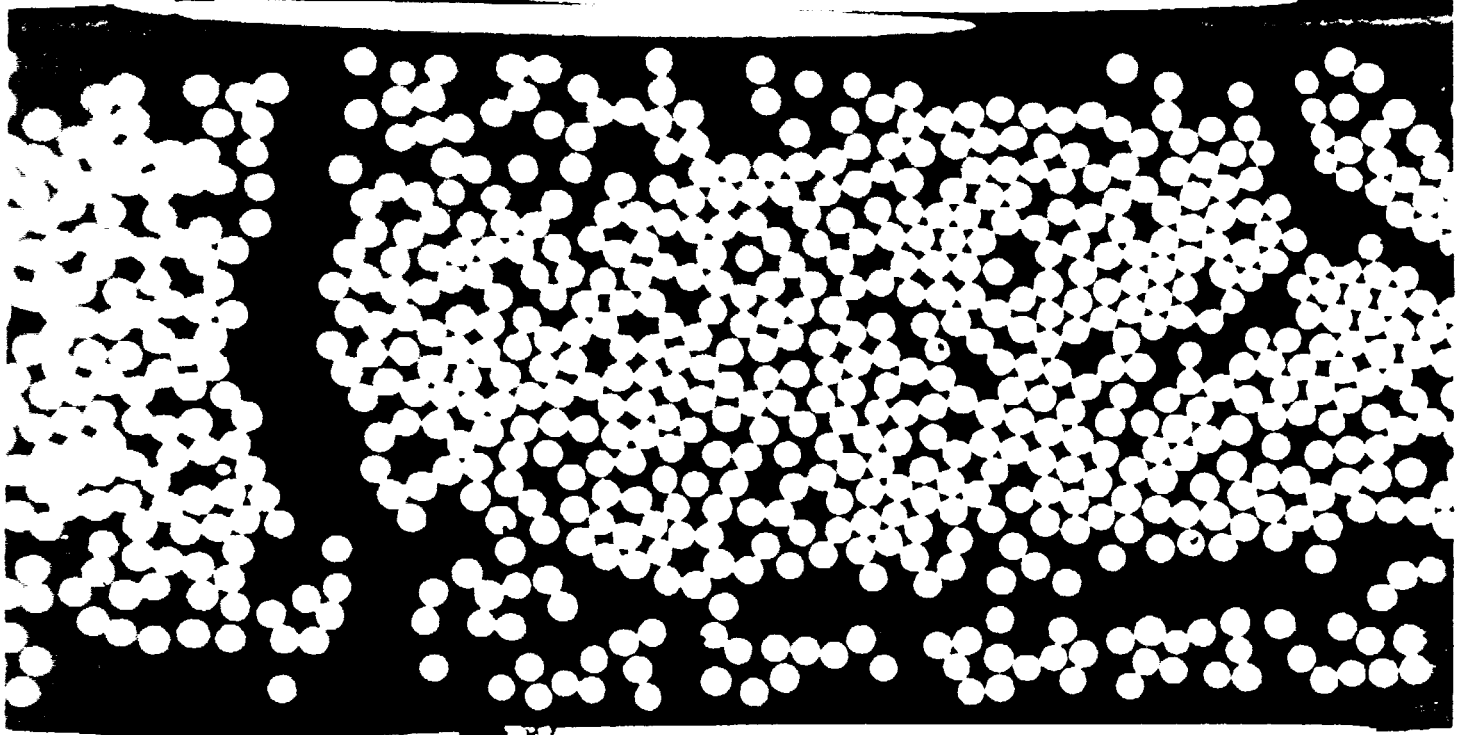


FIGURE 10b.



FIGURE 11.

ORIGINAL PAGE IS  
OF POOR QUALITY

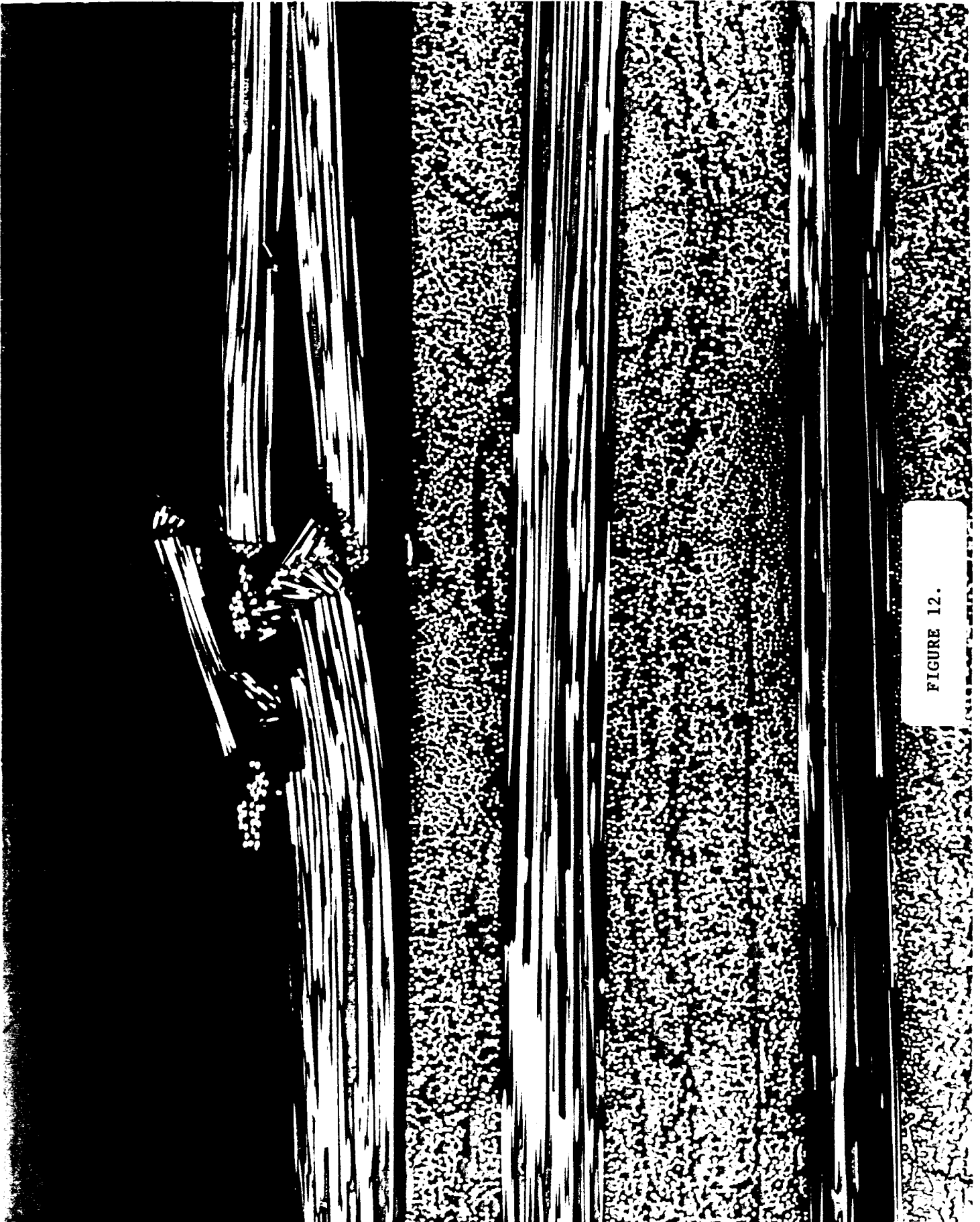


FIGURE 12.